



Hydrogen in aluminum

H.K. Birnbaum^{a,*}, C. Buckley^a, F. Zeides^a, E. Sirois^a, P. Rozenak^a, S. Spooner^b, J.S. Lin^b

^aMaterials Research Laboratory, University of Illinois, Urbana, IL USA

^bOak Ridge National Laboratory, Division of Metals and Ceramics, Oak Ridge, TN USA

Abstract

The introduction of solute hydrogen in high purity aluminum has been studied using a variety of experimental techniques. Very large hydrogen concentrations were introduced by electrochemical charging and by chemical charging. Length change and lattice parameter measurements showed that the hydrogen was trapped at vacancies which entered in a ratio close to $C_v/C_H=1$. Small angle X-ray scattering showed that the hydrogen-vacancy complexes clustered into platelets lying on the {111}.

Keywords: Aluminum; Hydrogen; Vacancies; Small angle scattering; Hydrogen-vacancy complex

1. Introduction

While various aspects of hydrogen in aluminum have been studied, there is still very little understanding of the state of hydrogen in the Al matrix. The solubility of H in Al is very low [1,2] and the enthalpy of solution has been experimentally measured as relatively low ($64.5 \text{ kJ mole}^{-1}$ [3]) or high (146 kJ mole^{-1} [2]) and has been theoretically calculated as 125 kJ mole^{-1} [4]. The configuration of the solute H atoms is presently unknown. It may occupy the normal tetrahedral interstitial sites but has been suggested to be associated with a lattice vacancy [4,5] where the calculations show that it sits off center near the tetrahedral site [6]. The binding enthalpy of the H-vacancy complex has been calculated to be 50 kJ mole^{-1} which also agrees with experimental measurements [7,8].

Uncertainty also exists in the results of hydrogen diffusion measurements in Al which show large scatter. Reported values of D_0 range from 4.6×10^{-6} to $1.2 \times 10^{-9} \text{ m}^2 \text{ s}^{-1}$ and the diffusion enthalpies vary between 36.6 to $139.5 \text{ kJ mole}^{-1}$ [2,9–12]. The suggestion that observed deviations from classical Arrhenius diffusion behavior is due to H-vacancy interactions was made [11] and was discounted by Ishikawa and McLellan [12] based primarily on the fact that the low temperature diffusion measurements agreed with those at high temperatures.

Strong evidence for the introduction of very high concentrations of vacancies and for hydrogen-vacancy interactions has been obtained at high temperatures and high hydrogen pressures in Ni, Pd, and Fe [13–15].

Vacancy concentrations of up to 20% have been reported in Ni where it was suggested [13] that these defects are a consequence of the very high binding enthalpies for the vacancy-6H complex [16].

In the present paper a summary of results obtained at high concentrations of H in high purity aluminum is given. These results, obtained at room temperature, strongly suggest that the solution of about 1000 atomic parts per million (appm) H in Al results in the formation of an equal concentration of vacancies.

2. Experimental procedures

Specimens having suitable configurations were cut from 99.999% pure aluminum. The only impurities detected by mass spectroscopic analysis was Si, Fe and Cu at levels of less than 2 ppm. For some experiments, specimens were cut from single crystals grown from the 99.999% Al in vacuum by a Bridgeman technique. The cutting was by spark erosion and was followed by careful polishing to minimize the damage to the surfaces. Specimens used for small angle scattering measurements were $70 \mu\text{m}$ in thickness. They were given a final anneal at 833 K in a vacuum of 10^{-4} Pa . Other experiments utilized polycrystalline sheets having thicknesses of 0.1–0.5 mm. All of the polycrystalline material was well annealed in a vacuum of 10^{-4} Pa .

Hydrogen charging was carried out using three methods—electrolytic charging in H_2SO_4 or HCl, using NaAsO_2 as a hydrogen recombination “poison”; by etching in NaOH (pH 10–12) containing NaAsO_2 as a

*Corresponding author.

hydrogen recombination “poison”; and by exposure to an ultrasonic field in a 125 W ultrasonic water bath. The electrolytic charging utilized a Pt anode and current densities of 1–200 mA cm⁻² as specified in Section 3. The details of these charging procedures will be discussed as required in Section 3. In cases where charging with deuterium was desired, D₂O, and D₂SO₄ was substituted for the corresponding H bearing component.

H(D) analysis was carried out using a vacuum extraction technique with the amount of H₂(D₂) released being determined by gas chromatography. The sensitivity of the method was about 1 appm. The distribution of the H(D) below the surface through which it was charged was measured by a Cameca secondary ion imaging mass spectrometer which had a depth resolution of about 10 nm. The initial H(D) distribution beneath the surface was not expected to be uniform due to the low temperature charging methods. However, the diffusivity of H measured at room temperature [12] is 2×10^{-14} m² s⁻¹ and the hydrogen should achieve a homogeneous distribution in the specimens used in $<3 \times 10^4$ s (500 min).

Length change measurements were made during hydrogen charging using both optical measurements and linear variable differential transformers (LVDT). Length change measurements were made along the length of the sheet specimens while the hydrogen entered through the lateral surfaces only. The estimated precision of the $\Delta L/L$ measurements is $\sim 5 \times 10^{-7}$ (for the LVDT measurements). Lattice parameter measurements were made immediately after charging using step scans of the X-ray peaks obtained with Cu K α radiation. The lattice parameters calculated from lines at various Bragg angles, θ , were extrapolated vs. $\cos^2 \theta / \sin \theta$ to increase the precision of measurement of $\Delta a/a$; which was estimated to be 10^{-4} .

Small angle X-ray scattering (SAXS) measurements were carried out using a parallel 1 mm² beam of Cu K α radiation in a 10 m camera fitted with an area detector and heating and double axis tilting stages. The area detector

has a 20×20 cm² active area with a resolution of 6.25×10^{-4} radians at a sample to detector distance of 5 m. Thin, single crystal plates of 70 μ m thickness and oriented with the $\langle 110 \rangle$ normal to the face of the crystals were used. They were prepared by careful spark erosion cutting of oriented crystals followed by hand polishing in a holder designed to maintain their orientation. Care was taken to avoid the introduction of H during the polishing, e.g., contact with water was avoided during the polishing. Specimens for SAXS were electrolytically charged with H, with the H concentration being measured on identical samples charged in parallel with the samples used for SAXS measurements. Subsequent to the charging and aging at room temperature, the surfaces were examined in the scanning electron microscope (SEM) at magnifications up to 2×10^4 and no indication of surface roughening or bubbles was observed. These measurements are still being analyzed and only preliminary results will be described in this paper.

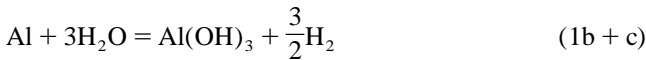
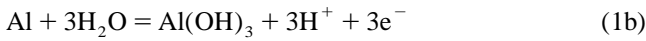
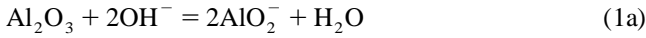
3. Results and discussion

The solubility of H in Al in equilibrium with 1 atm. of H₂ gas at 660 K (i.e., at the melting point) [1] results in about 1 appm in solid solution. The solubility at 300 K is very much smaller. All of the chemical and electrolytic charging methods used resulted in C_H of the order of 1000 appm suggesting that they correspond to very high fugacity charging methods. Cathodic charging in aqueous solutions of H₂SO₄ and HCl are known to result in high H fugacities and while most of the H comes off as H₂ bubbles, in the presence of the recombination poison, NaAsO₄, about 600–2000 appm of H is entered into solution as shown in Table 1. In these specimens, no significant degradation of the surfaces was observed suggesting that the transport of H into the specimen occurs across the coherent thin Al₂O₃ oxide on the surface.

Table 1
Hydrogen charging of high purity aluminum

Charging conditions	C_H (appm)	$\Delta L/L_0$	$\Delta a/a_0$	C_v (calc)	$\frac{C_v}{C_H}$	$(\Delta L/L_0)$ H only
Cathodic charging						
H ₂ SO ₄ + NaAsO ₄ , pH 2; 35 C, 1.7 mA cm ⁻²	1090	$+2.7 \times 10^{-6}$		3.7×10^{-4}	0.28	$+6.4 \times 10^{-5}$
HCl + NaAsO ₄ , pH 1.5; 35 C, 1.7 mA cm ⁻²	675	$+6.6 \times 10^{-6}$		2.0×10^{-4}	0.29	$+3.9 \times 10^{-5}$
1 N H ₂ SO ₄ + NaAsO ₄ , pH 1; 35 C, 50 mA cm ⁻²	2000		-1.7×10^{-4}	1.7×10^{-3}	0.85	$+1.1 \times 10^{-4}$
1 N D ₂ SO ₄ (D ₂ O) + NaAsO ₄ , pH 1; 35 C, 200 mA cm ⁻²	900					
Chemical charging						
1 N NaOH; pH 12	600		-3.3×10^{-4}	2.3×10^{-3}	3.7	$+3.4 \times 10^{-5}$
1 N NaOH; saturated with Al; pH 12	1300	-3×10^{-4}		2.3×10^{-3}	1.8	$+7.3 \times 10^{-5}$
Ultrasonic bath						
D ₂ O; 6 hours	2500					
H ₂ O; \sim 10 hours	1300					

Aqueous solutions of NaOH are known to be aggressive towards aluminum and chemical charging at pH 12 resulted in dissolution of the Al as well as introduction of H at concentrations of 600–1300 appm as shown in Table 1. It is suggested that the introduction of solute H results from the reaction of Al with H₂O and that the alkaline solution serves to remove the Al₂O₃ allowing the reaction of the Al and H₂O. This reaction path is described by:



At 300 K the free energy of reaction (b+c) is $\Delta G_{b+c} = -430.1 \text{ kJ mole}^{-1}$ which leads to an equilibrium constant of $K_{b+c} = 1.36 \times 10^{75}$. Since the latter is given by:

$$K_{b+c} = (f_{\text{H}_2})^{3/2} \quad (2)$$

this results in a value for hydrogen fugacity of $f_{\text{H}_2} = 1.3 \times 10^{50} \text{ atm.}$

The H fugacity corresponding to the concentrations observed after cathodic charging in acids, or chemical charging in aqueous NaOH, can be estimated from the high temperature solubility measurements [17] which give values of:

$$\log s = \frac{2080}{T} + 0.788 + \frac{1}{2} \log f_{\text{H}_2} \quad (3)$$

where s is the hydrogen solubility in units of $\text{cm}^3 (\text{H}_2)/ (100 \text{ g Al})$. For the H concentrations introduced by charging ($\sim 1300 \text{ appm}$), s corresponds to $53.54 \text{ cm}^3 (\text{H}_2)/ (100 \text{ g Al})$ and the $f_{\text{H}_2} \sim 10^{15} \text{ atm.}$ Comparing this to the f_{H_2} obtained from the reaction of Al and H₂O, it is clear that the chemical reaction is more than sufficient to introduce the measured H concentrations. Similarly, the overvoltage ($E_{\text{overpotential}}$) required to achieve $f_{\text{H}_2} \sim 10^{15} \text{ atm.}$ in the cathodic charging is $\sim 0.47 \text{ V}$ and the voltage used in the electrochemical cell exceeds this by a considerable amount.

Confirmation that reaction (1c) provides sufficient H fugacity to achieve the H concentrations observed is obtained from the charging experiments in an aqueous ultrasonic bath (Table 1). In this case the sonic field disrupts the surface oxide and allows reaction (1b+c) to occur. The fugacity obtained is about that obtained when the Al₂O₃ is dissolved by NaOH solutions, and the H concentrations obtained are comparable.

Introduction of H into the lattice of fcc solids generally results in a considerable lattice expansion [18] with almost all of the systems exhibiting a volume expansion of $\delta V_{\text{H}} = 0.28 \text{ nm}^3$. For the atomic volume of Al (Ω) this corre-

sponds to $\delta V_{\text{H}}/\Omega = 0.168$ per H atom. Table 1 shows the expected length (lattice parameter) change, $(\Delta L/L_0)_{\text{H only}} = (\Delta a/a_0)_{\text{H only}}$, expected for the solute H for each of the charging conditions used. In general, lattice expansions of the order of $+5 \times 10^{-5}$ are expected. In contrast, the measured values of $\Delta L/L_0$ and $\Delta a/a_0$ (Table 1) are either significantly smaller expansions or are negative, i.e., a contraction of the lattice. In both cases, the results suggest that the lattice expansion is greatly less in Al than in other metals.

These results can be accounted for by the formation of a lattice vacancy at the surface accompanying the introduction of a H solute followed by the diffusion of the H-vacancy complex into the volume. In this model, the vacancies are formed at the external surfaces and the additional lattice sites formed are introduced at the external surfaces rather than at internal vacancy sources. Since the length changes are measured along a direction in which no additional lattice sites are created, the measured $\Delta L/L_0$ is determined only by the relaxation volume around the vacancy, δ_v , rather than by the entire formation volume of the vacancy, $\delta_v + \Omega$. In the situation where the H-vacancy complexes remain dispersed as individual defects, the volume change is:

$$\begin{aligned} \Delta a/a_0 &= \Delta L/L_0 = \frac{1}{3}(\Delta V/V_0) \\ &= \frac{1}{3}(C_{\text{H}}[\delta_{\text{H}}/\Omega] + C_{\text{v}}[\delta_{\text{v}}/\Omega]) \end{aligned} \quad (4)$$

where C_{v} is the concentration of vacancies and $\delta_{\text{v}}/\Omega = -0.49$ is the magnitude of the lattice relaxation due to a vacancy in Al [19]. From Eq. (4), the values of C_{v} and $C_{\text{v}}/C_{\text{H}}$ can be calculated and are shown in Table 1. While there is considerable scatter in the results, the observed low values of lattice expansion can be accounted for by values of $C_{\text{v}}/C_{\text{H}}$ between about 0.25 and 4 with the highest values of the vacancies being introduced under the most aggressive H charging conditions. As will be seen shortly, there is evidence that the H-vacancy complexes do not remain as single defects but rather cluster into platelets. Clustering would result in an increase in the observed values of $(\Delta a/a_0)$ and $(\Delta L/L_0)$ and hence in a decrease in the calculated values of $C_{\text{v}}/C_{\text{H}}$ (Table 1) relative to that which would be observed, had the H-vacancy defects remained dispersed.

The binding enthalpy of the H-vacancy complex, B_{Hv} , has been calculated to be 50 kJ mole^{-1} [20] which also agrees with experimental measurements [7,8]. Since the vacancy formation enthalpy in Al, H_{v}^{f} , has been determined to be $63.5 \text{ kJ mole}^{-1}$ [21], the formation of the H-vacancy complex has a very large effect on the vacancy population in the Al. Since the formation of vacancies in the presence of H can be written as:

$$C_{\text{v}} = \exp(-[H_{\text{v}}^{\text{f}} - B_{\text{Hv}}]/RT) \quad (5)$$

for $C_{\text{v}} = C_{\text{H}} = 10^{-3}$ at 300 K, B_{Hv} can be estimated to be

46.1 kJ mole⁻¹, in good agreement with the previous theoretical calculations and experimental results. This value is also in good agreement with the H-vacancy binding enthalpy obtained from high temperature permeation measurements of H in Al [11] where it was shown that the H diffuses as a H-vacancy complex.

The degree and nature of the agglomeration of the H-vacancy complexes in Al are being studied with SAXS and small angle neutron scattering (SANS). Results are available for the SAXS measurements but these are only partially analyzed. SAXS measurements of 70 μm thick specimens which were electrolytically charged with about 1000 appm H and aged at room temperature for several weeks showed SAXS patterns similar to that shown in Fig. 1. For this pattern the X-ray beam was normal to the surface and was along the [110]. The scattering patterns were highly anisotropic and exhibited extended streaking along the [1 $\bar{1}$ 1] and [$\bar{1}$ 11]. Uncharged, well annealed specimens did not exhibit any significant small angle scattering for the [110] crystal orientation. The observed anisotropic intensity distribution is consistent with scattering from platelets lying on the {111}. Since H has a negligible X-ray scattering factor, it is concluded that the most likely defect is vacancy plates lying on the {111}. While additional experiments, including critical tilting experiments are required, the initial data was analyzed using the Guinier scattering law [22]:

$$\ln I(q) = -R_g^2 q^2/3 + \text{constant}; R = (5/3)^{0.5} R_g \quad (6)$$

where $I(q)$ is the scattered intensity, $q=4\pi \sin \theta)/\lambda$, R_g is the electronic radius of gyration, and R is the geometric radius of the defects. As a first approximation, the log $I(q)$ was plotted vs. q^2 for the intensities taken along the streaks

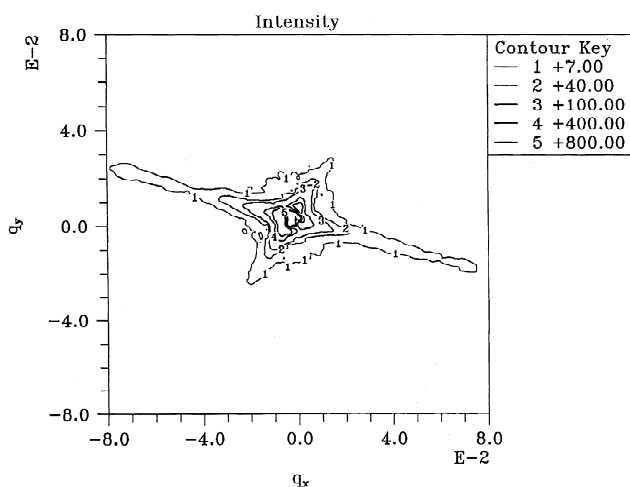


Fig. 1. Small angle X-ray scattering from Al electrolytically charged with 1000 appm H from 1 N H₂SO₄ at a current density of 50 mA cm². The Cu K_α X-ray beam was oriented along the [110]. The scattering streaks were oriented along the [1 $\bar{1}$ 1] and [$\bar{1}$ 11]. The contour lines correspond to count rates of 800 c s⁻¹ to 7 c s⁻¹. The actual highest count rate was ~1800 c s⁻¹.

in the <111>. From the slopes at $q=0$, the streaks can be interpreted as plate-like defects having a radius of 15 nm and from the slopes at large q having a thickness of about 7 nm. The scattered intensity $I(0)$ at $q=0$ is given by:

$$\Delta V/V = I(0)/\pi R^2 t [\Delta\Omega]^2 \quad (7)$$

where $\Delta V/V$ is the volume fraction of platelets, R is the radius and t the thickness of the platelets, and $\Delta\Omega=0.79$ is the electron density difference between the platelets and the matrix. Applying Eq. (7) to the scattering data yields $\Delta V/V=2\times 10^{-5}$.

Annealing experiments were carried out on the specimens which showed the anisotropic scattering. Isochronal annealing to 573 K showed a decrease in the intensity of the anisotropic scattering but the streaks along the <111> were still present although attenuated in length. Annealing to 773 K left only isotropic scattering with greatly diminished intensity indicating that the H-vacancy platelets had dispersed to individual defects. On cooling to 300 K the anisotropic pattern was recovered both in intensity and in the extent of the anisotropy suggesting that the H-vacancy defects clustered once again. At the elevated temperatures the fraction of the H-vacancy defects which have dissociated can be calculated from B_{Hv} yielding $C_{Hv}/C_v \sim 2.5$ at 772 K. The dispersal of the H-vacancy defects from the platelets at high temperatures leaves the H trapped at individual vacancies and the H-vacancy defects can then cluster on cooling.

4. Conclusions

1. Hydrogen concentrations of the order of $C_H \sim 0.001$ can be introduced into Al by cathodic charging or by reaction of Al with H₂O when the Al₂O₃ is removed by NaOH or ultrasonic fields in aqueous solutions.

2. Hydrogen enters Al accompanied by a vacancy formed at the surface. The H-vacancy binding enthalpy is about 46.1 kJ mole⁻¹ in good agreement with previous measurements and theory.

3. The H-vacancy defects form platelets lying on the {111} and having sizes of about 15 nm radius and 7 nm thickness. These platelets are present in concentrations of about $\Delta V/V \sim 2\times 10^{-5}$. The platelets are stable on heating to about 773 K and reform on cooling to 300 K.

Acknowledgments

This work was supported by the Department of Energy, Division of Materials Sciences through Grant DEFG02-96ER45439 at the Materials Research Laboratory and Grant DE-AC05-96OR22464 at Oak Ridge National Laboratory which is managed by Lockheed-Martin Energy Research Company.

References

- [1] W. Eichenauer, *Z. Metallkunde*, *59* (1968) 613.
- [2] M. Ichimura, Y. Sasajima, M. Imabayashi and H. Katsuta, *J. Phys. Chem. Solids*, *49* (1988) 1259.
- [3] R.A. Edwards and W. Eichenauer, *Scripta Metall.*, *14* (1980) 971.
- [4] D.S. Larsen and J.K. Nørskov, *J. Phys. F, Met. Phys.*, *9* (1979) 175.
- [5] S.M. Meyers, F. Besenbacher and J.K. Nørskov, *J. Appl. Phys.*, *58* (1985) 1841.
- [6] J.P. Bugeat, A.C. Chamie and E. Ligeon, *Phys. Lett.*, *A58* (1976) 127.
- [7] S.M. Myers, F. Besenbacher and J.K. Nørskov, *J. Appl. Phys.*, *58* (1985) 1841.
- [8] S. Linderöth, H. Rajainmaki and R.M. Nieminen, *Phys. Rev.*, *B35* (1987) 5524.
- [9] R.B. McLellan, *Scripta Metall.*, *17* (1983) 1237.
- [10] R.A. Outlaw, *Scripta Metall.*, *16* (1982) 287.
- [11] E. Hashimoto and T. Kino, *J. Phys. F, Met. Phys.*, *13* (1983) 1157.
- [12] T. Ishikawa and R.B. McLellan, *Acta Metall.*, *34* (1986) 1091.
- [13] Y. Fukai and N. Okuma, *J. Appl. Phys.*, *32* (1993) 1256.
- [14] Y. Fukai, M. Yamakata and T. Yagi, *Z. Phys. Chem.*, *179* (1993) 119.
- [15] Y. Fukai and N. Okuma, *Phys. Rev. Lett.*, *73* (1994) 1640.
- [16] S.M. Myers, P. Nordlander, F. Besenbacher and J.K. Nørskov, *Phys. Rev.*, *B33* (1986) 854.
- [17] C.E. Ransley and H. Neufeld, *J. Inst. Metals*, *74* (1948) 599.
- [18] H. Peisl, in G. Alefeld and J. Volkl (eds.), *Hydrogen in Metals I, Topics in Applied Physics*, Vol. 28, Springer Verlag, Berlin, 1978, pp. 53–74.
- [19] K.M. Miller and P.T. Heald, *Phys. Status Solidi (b)*, *67* (1975) 569.
- [20] F. Besenbacher, S.M. Myers and J.K. Nørskov, *Nucl. Instrum. Methods Phys. Res. B*, *7/8* (1985) 55.
- [21] R.W. Siegel, *J. Nucl. Mater.*, *69–70* (1978) 117.
- [22] A. Guinier and G. Fournet, *Small Angle Scattering of X-Rays*, Wiley, New York, 1955.